

## Gaussian Process Modeling of Protein Turnover

Mahbubur Rahman<sup>1,2</sup>, Stephen F. Previs<sup>3</sup>, Takhar Kasumov<sup>4,5</sup>, and Rovshan G. Sadygov<sup>1,2,\*</sup>

<sup>1</sup>Department of Biochemistry and Molecular Biology, <sup>2</sup>Sealy Center for Molecular Medicine, The University of Texas Medical Branch, Galveston, Texas 77555

<sup>3</sup>Merck Research Laboratories

2015 Galloping Hill Road

Kenilworth, NJ 07033

<sup>4</sup>Department of Gastroenterology & Hepatology, Cleveland Clinic

Cleveland, OH 44195

<sup>5</sup>Department of Pharmaceutical Sciences

School of Pharmacy, Northeast Ohio Medical University

Rootstown, OH 44225

\*To whom correspondence should be addressed: Tel. 409-772-3287; Fax 409-772-9670; email: rovshan.sadygov@utmb.edu

### Abbreviations:

GP, Gaussian Process; LC-MS, ODE, ordinary differential equation; OU, Ornstein-Uhlenbeck.

### Table of Contents:

1. Derivation of the GP Model from the Stochastic Differential Equation of Protein Turnover Kinetics
2. Diagram D1, one- and two-compartment models of protein turnover.
3. Figure S1 – pairwise scatter plot of the residual sum of squares for mouse brain proteins;
4. Figure S2 – the pairwise scatter plots of the Pearson correlations obtained from GP and two-exponent curve fitting for mouse liver
5. Figure S3 – the pairwise scatter plots of the Pearson correlations obtained from GP and two-exponent curve fitting for mouse brain proteins.
6. Figure S4 – 95% confidence interval of the mean of GP model for mitochondrial trifunctional protein, subunit  $\alpha$  (Q8BMS1);

7. Figure S5 – the scatter plot of the decay rates constants obtained from the GP and two-exponent curve fitting for mouse brain proteins;
8. Figure S6 – the density of the difference between degradation rate constants computed by the GP and two-exponent curve fitting;
9. Figure S7 – the boxplots of decay rate constants computed by two-exponent curve fitting and GP model for mouse brain and liver proteomes;
10. Figure S8 –the density of standard deviations of the model distributions for mouse liver proteins;

## Derivation of the GP Model from the Stochastic Differential Equation of Protein Turnover Kinetics

The kinetic equations for protein turnover dynamics are derived under the condition of steady-state that is the total protein abundance,  $P$ , at any time is constant:

$$P(t) = P(t)^H + P(t)^L = \text{const}$$

where,  $P(t)^H$  and  $P(t)^L$  denote the heavy (stable isotope labeled) and light (natural) protein abundances, respectively. In the one-compartment model<sup>1</sup> it is assumed that the proteins are degraded proportional to their abundance with a rate constant,  $k_{\text{deg}}$ , and are synthesized at a constant rate  $k_{\text{syn}}$ . The Diagram 1 A shows the one-compartment. The kinetic equations for the heavy isotope labeled proteins,  $P(t)^H$ , and unlabeled proteins,  $P(t)^L$  are:

$$\begin{cases} \dot{P}(t)^H = -k_{\text{deg}}P(t)^H + k_{\text{syn}} \\ \dot{P}(t)^L = -k_{\text{deg}}P(t)^L \end{cases}$$

(1a)

Eq. (1A) assumes that the labeling is 100% and asymptotically only labeled proteins will be present in the sample. However, in general, the labeling is not 100% for all proteins. To account for this, we consider a possibility that only a portion of proteins,  $\lambda$ , is labeled asymptotically, while the rest  $(1 - \lambda)$  are unlabeled. The new set of equations for the protein concentrations becomes:

$$\begin{cases} \dot{P}(t)^H = -k_{\text{deg}}P(t)^H + \lambda k_{\text{syn}} \\ \dot{P}(t)^L = -k_{\text{deg}}P(t)^L + (1 - \lambda)k_{\text{syn}} \end{cases}$$

(1b)

Since Eq. (1a) is particular case of Eq. (1b), in the rest of the text we will use the latter to develop our model. The total protein concentration,  $P(t)$ , is assumed to be in a steady-state and the relevant kinetic equation is:

$$P\dot{(t)} = -k_{deg}P(t) + k_{syn} = 0$$

From the above equation we obtain  $k_{syn}$ :

$$k_{syn} = k_{deg}P(t)$$

(1c)

The ratio of the synthesis rate over protein concentration is a convenient measure to estimate the fraction of the newly synthesized protein. This measure, termed the fractional synthesis rate, is equal to the degradation rate constant under the steady-state assumption, Eq. (1c). When we insert the above value of  $k_{syn}$  into the kinetic equation for  $P(t)^H$  in Eq. (1b), and divide left- and right-hand sides of the equation by  $P(t)$ , then we obtain differential equation for  $\beta(t) = P(t)^H/P(t)$ , proportion of the protein that has incorporated heavy isotopes:

$$\beta\dot{(t)}^H = -k_{deg}\beta(t) + \lambda k_{deg} = k_{deg}(\lambda - \beta(t))$$

(2)

The solution to Eq. (2) is obtained, for example, by the variation of constants, first solving the equation without the  $\lambda k_{deg}$  term, to obtain,  $\beta(t) = Ce^{-k_{deg}t}$ . Then by inserting the solution into Eq. (2) and allowing the variation of  $C$ , we obtain the equation for  $C$ :

$$C\dot{(t)}e^{-k_{deg}t} = \lambda k_{deg}$$

which produces a solution for  $C(t)$ :

$$C(t) = \lambda e^{k_{deg}t} + C_0$$

where  $C_0$  is a constant. The solution of  $\beta(t)$  is then,

$$\beta(t) = \lambda + C_0 e^{-k_{\text{deg}} t}$$

The value of  $C_0$  is obtained from the initial condition. It is assumed that at time  $t = 0$ , there were no heavy isotope labeled proteins and therefore  $\beta(0) = 0$ :

$$\beta(t) = \lambda(1 - e^{-k_{\text{deg}} t})$$

(3)

Eq. (3) is the solution for the proportion of the heavy isotope labeled proteins in one-compartment model.

A general form of the stochastic analog of Eq. (2) for the heavy protein proportions is:

$$dX(t) = k_{\text{deg}}(\lambda - X(t))dt + \Gamma(k_{\text{deg}}, t, X, \lambda, \sigma_\gamma)dB(t), \quad X(0) = 0$$

where  $\Gamma(k_{\text{deg}}, t, X, \lambda, \sigma_\gamma)$  is the volatility,  $dB(t)$  is the Brownian motion,  $\sigma_\gamma$  is the standard deviation of model fluctuations, and  $X(t)$  is the stochastic equivalent of  $\beta(t)$ . We chose a homoscedastic volatility, with the volatility equal to the standard deviation,  $\Gamma(k_{\text{deg}}, t, X, \lambda, \sigma_\gamma) = \sigma_\gamma$ . As it will be seen below, the choice of  $\Gamma$  leads to a Gaussian Process (GP) for  $X(t)$ . If we have used an affine volatility function,  $\Gamma(k_{\text{deg}}, t, X, \lambda, \sigma_\gamma) = X(t)\sigma_\gamma$ , the process,  $X(t)$ , will then be a log-Gaussian process<sup>2</sup>.

With the  $\Gamma(k_{\text{deg}}, t, \beta, \sigma_\gamma) = \sigma_\gamma$  the equation for  $X(t)$  becomes:

$$dX(t) = k_{\text{deg}}(\lambda - X(t))dt + \sigma_\gamma dB(t), \quad X(0) = 0$$

(4)

The solution to Eq. (4) is found with the assumption of the Itô's process<sup>3</sup> for  $X(t)$ . In this case, a function,  $Z(t)$ , defined as:

$$Z(t) = X(t) e^{tk_{\text{deg}}}$$

(5)

Using the Itô's formulae<sup>3</sup>

$$dZ(t) = \left( \frac{\partial}{\partial X} Z(t) \right) dX(t) + \left( \frac{\partial}{\partial t} Z(t) \right) dt + \left( \frac{\partial^2}{\partial X^2} Z(t) \right) (dX(t))^2$$

we find that

$$Z(t) = X(0)e^{0 \cdot k_{\text{deg}}} + \int_0^t e^{sk_{\text{deg}}} \{k_{\text{deg}}(\lambda - X(s))ds + \sigma_Y dB(s)\} + k_{\text{deg}} \int_0^t e^{sk_{\text{deg}}} X(s)ds$$

and after some straightforward simplifications we obtain:

$$Z(t) = \lambda(e^{tk_{\text{deg}}} - 1) + \sigma_Y \int_0^t e^{sk_{\text{deg}}} dB(s)$$

Inserting the formulae for Z(t) back into Eq. (5) yields the solution for X(t):

$$X(t) = \lambda(1 - e^{-tk_{\text{deg}}}) + \sigma_Y \int_0^t e^{-k_{\text{deg}}(t-s)} dB(s)$$

(6)

The stochastic process in Eq. (6) is well-known GP with Ornstein-Uhlenbeck (OU) covariance matrix<sup>3, 4</sup>, K(s,t), defined as:

$$K(s, t) = \sigma_Y^2 e^{(-|s-t|k_{\text{deg}})} / k_{\text{deg}}$$

and the mean,  $\mu(t)$ :

$$\mu(t) = (1 - e^{-tk_{\text{deg}}})\lambda$$

If in addition to the correlated noise there is also a white noise corresponding to errors in measurements ( $\varepsilon \sim N(0, \sigma_\varepsilon^2)$ ), then the final process, Y(t), is:

$$Y(t) = X(t) + \varepsilon; \quad \vec{Y} \sim \text{MVN}(\vec{\mu}, \Sigma); \quad \Sigma(s, t) = K(s, t) + \sigma_\varepsilon^2 \delta(s, t); \quad \vec{Y}, \vec{\mu} \in \mathbb{R}^N; \quad \Sigma, K \in \mathbb{R}^{N \times N}$$

is a GP with the covariance matrix  $\Sigma(s, t)$ . Here, MVN stands for multivariate normal distribution, n is the number of data (time) points,  $\vec{Y}$  and  $\vec{\mu}$  are vectors in an n dimensional space,  $\mathbb{R}^n$ , and  $\delta$  is the Kronecker's delta.

We note that in an earlier publication, a solution for Eq. (6) was applied with a Gaussian kernel in phospho-protein time course data analysis<sup>1, 5</sup>. The Gaussian kernel

has two parameters: the scale, and the strength. The decay/rate constant is a separate parameter. All three parameters have to be determined from the fits to experimental data. In the OU kernel, the scale parameter is the degradation rate constant and therefore there is one less parameter. It is an important consideration, as in addition being an exact solution, a model with reduced number of parameters are less likely to overfit the data.

Many bioinformatics software<sup>1, 6</sup> to extract protein degradation rates from the stable isotope labeling mass spectrometric experiments used one or other form of the solution to Eq. (3) (with the assumption that  $\lambda = 1$ ). However, in an depth analysis of a large-scale dataset from a <sup>15</sup>N labeling of mouse, Guan and colleagues<sup>1</sup> have shown that the model is not adequate for most of the proteins, in particular in the cases of fast protein turnover. A natural extension of the model is the two-compartment model, where in addition to the protein decay and synthesis, amino acid decay and synthesis are also considered. The Diagram 1 B shows the two-compartment models. The assumptions results in the following kinetic equations for  $P(t)^H$  and  $AA(t)^H$ , the concentration of the labeled amino acids in the precursor pool:

$$\begin{cases} \dot{P}(t)^H = k_{syn}AA(t)^H - k_{deg}P(t)^H \\ \dot{AA}(t)^H = \lambda k_0 - k_{syn}AA(t)^H \end{cases} \quad (7)$$

where  $k_0$  is the constant rate of amino acid synthesis, and the model incorporates incomplete labeling of amino acids, and subsequently proteins. The system of equations (7) for labeled species concentrations is first transformed into the corresponding system of equations for the proportions of the labeled species:

$$\begin{cases} \dot{\beta}(t) = k_{\text{deg}}\alpha(t) - k_{\text{deg}}\beta(t) \\ \dot{\alpha}(t) = \lambda k_{\text{syn}} - k_{\text{syn}}\alpha(t) \end{cases} \quad (8)$$

where  $\alpha(t) = \frac{AA(t)^H}{AA}$ , and AA denotes the concentration of amino acids. The kinetic equation for labeled proportion of amino acids,  $\alpha(t)$ , is obtained by observing that (in the steady-state approximation):

$$AA = AA(t)^H + AA(t)^L = \text{const}; \quad \dot{AA} = k_0 - k_{\text{syn}}AA = 0; \quad AAk_{\text{syn}} = k_0$$

The kinetic equation for  $\beta(t)$  is obtained similarly by observing that:

$$P = P(t)^H + P(t)^L = \text{const}; \quad \dot{P} = k_{\text{syn}}AA - k_{\text{deg}}P = 0; \quad Pk_{\text{deg}} = k_{\text{syn}}AA;$$

$$k_{\text{syn}}AA(t)^H = \alpha(t)k_{\text{syn}}AA = \alpha(t)k_{\text{deg}}P$$

By inserting the expressions for  $k_{\text{syn}}AA(t)^H$  and  $k_0$  into the first and second equations in (7), we obtained the system of equations (8).

The solution for  $\alpha(t)$  is obtained using the variation of constants (similar to the solution (3)), and the initial condition ( $\alpha(0) = 0$ ):

$$\alpha(t) = \lambda(1 - e^{-tk_{\text{syn}}})$$

Inserting the result into Eq. (8) for  $\beta(t)$  we obtain the kinetic equation for it:

$$\dot{\beta}(t) = \lambda k_{\text{deg}}(1 - e^{-tk_{\text{syn}}}) - k_{\text{deg}}\beta(t)$$

(9)

One way to solve the equation is to again use the variation of constants:

$$\dot{\beta}(t) = -k_{\text{deg}}\beta(t); \quad \beta(t) = Ce^{-k_{\text{deg}}t}$$

Then the equation for C(t) is:

$$C(t)e^{-k_{\text{deg}}t} = \lambda k_{\text{deg}}(1 - e^{-tk_{\text{syn}}})$$

$$C(t) = C_0 + \lambda e^{tk_{\text{deg}}} + \frac{\lambda k_{\text{deg}}}{k_{\text{syn}} - k_{\text{deg}}} e^{-(k_{\text{syn}} - k_{\text{deg}})t}$$



And  $\beta(t)$  is:

$$\beta(t) = C_0 e^{-k_{deg}t} + \lambda + \frac{\lambda k_{deg}}{k_{syn} - k_{deg}} e^{-k_{syn}t}$$

$C_0$  is obtained from the initial condition,  $\beta(0) = 0$ :

$$C_0 = -\lambda - \frac{\lambda k_{deg}}{k_{syn} - k_{deg}} = -\frac{\lambda k_{syn}}{k_{syn} - k_{deg}}$$

And for  $\beta(t)$ :

$$\beta(t) = \lambda - \lambda(k_{syn} e^{-tk_{deg}} - k_{deg} e^{-k_{syn}t}) / (k_{syn} - k_{deg})$$

Thus, the two-compartment model results in a two-exponent fit for the proportions of the labeled proteins.

The stochastic equation corresponding to Eq. (9) is:

$$dX(t) = k_{deg}(\lambda(1 - e^{-tk_{syn}}) - X(t)) + \sigma_\gamma dB(t), \quad X(0) = 0$$

(10)

where, similar to Eq. (4) we have assumed the homoscedasticity of volatility,

$$\Gamma(k_{deg}, k_{syn}, t, X, \lambda, \sigma_\gamma) = \sigma_\gamma.$$

The random process,  $X(t)$ , in Eq. (10) is obtained similar to (6), by considering a derived Itô's process,  $Z(t)$ , shown in Eq. (5) and using Itô's formulae:

$$Z(t) = \int_0^t e^{sk_{deg}} \{k_{deg}(\lambda(1 - e^{-sk_{syn}}) - X(s)) + \sigma_\gamma dB(s)\} + k_{deg} \int_0^t e^{sk_{deg}} X(s) ds$$

Straightforward integrating with the exponents results in:

$$Z(t) = \lambda(e^{tk_{deg}} - 1) - \lambda k_{deg}(e^{t(k_{deg} - k_{syn})} - 1) / (k_{deg} - k_{syn}) + \sigma_\gamma \int_0^t e^{sk_{deg}} dB(s)$$

Using Eq. (5) we obtain for the random process  $X(t)$ :

$$X(t) = \lambda(1 - e^{-tk_{deg}}) - \lambda k_{deg}(e^{-tk_{syn}} - e^{-k_{deg}t}) / (k_{deg} - k_{syn}) + \sigma_\gamma \int_0^t e^{-k_{deg}(t-s)} dB(s)$$

and after straightforward arithmetic,  $X(t)$  is the following process:

$$X(t) = \lambda - \lambda(k_{\text{syn}}e^{-tk_{\text{deg}}} - k_{\text{deg}}e^{-k_{\text{syn}}t}) / (k_{\text{syn}} - k_{\text{deg}}) + \sigma_{\gamma} \int_0^t e^{-k_{\text{deg}}(t-s)} dB(s)$$

(11)

The process in Eq. (11) is process in Eq. (6) and they both are GPs with OU kernel. The only difference is in the means which for Eq. (11) is:

$$\mu(t) = \lambda - \lambda(k_{\text{syn}}e^{-tk_{\text{deg}}} - k_{\text{deg}}e^{-k_{\text{syn}}t}) / (k_{\text{syn}} - k_{\text{deg}})$$

The final process,  $Y(t)$ , includes the white noise due to the instrumental measurements:

$$Y(t) = X(t) + \varepsilon; \quad \vec{Y} \sim \text{MVN}(\vec{\mu}, \Sigma); \quad \Sigma(s, t) = K(s, t) + \sigma_{\varepsilon}^2 \delta(s, t);$$

(12)

The OU kernel  $K(s, t)$  was defined above.

### Parameter Estimation

We used the random process (12) to fit the experimental data and extract the parameters,  $\theta = (k_{\text{deg}}, k_{\text{syn}}, \sigma_{\gamma}, \sigma_{\varepsilon}, \lambda)$ . The parameter estimation was done by maximizing the posterior distribution of the model parameters. The log-likelihood function for the process (12) is:

$$\log(\mathcal{L}(\theta)) = -0.5 \log(\det(\Sigma)) - 0.5(\vec{y} - \vec{\mu})^T \Sigma^{-1}(\vec{y} - \vec{\mu}) - 0.5n \log(2\pi)$$

In the above formula  $T$  stands for transpose. The  $\theta$  dependent part of the posterior distribution,  $p(\theta|y)$ , is the product of the likelihood function and the prior distributions,  $\pi(\theta)$ . The log of the posterior distribution of the parameters is:

$$\log(p(\theta|y)) \propto \log(\mathcal{L}(\theta)) + \log(\pi(\theta))$$

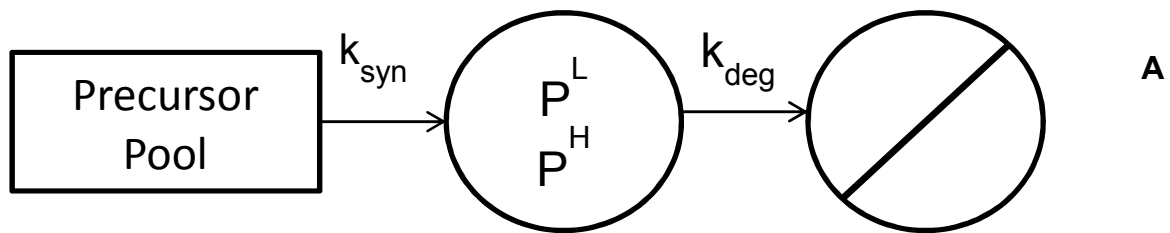
(13)

The parameters can be estimated from the data either by maximizing the posterior distribution, Eq. (13), with respect to the parameters<sup>7</sup>, or by sampling from the posterior distribution with Markov chain Monte Carlo methods<sup>8</sup>. We used a quasi-Newton approach<sup>9</sup> to maximize the posterior distribution function and obtain the parameters. For the prior distributions (except for  $\lambda$ ) we chose exponential distributions with the prior decay rates estimated from the non-stochastic model. For  $\lambda$  a uniform prior was chosen. To improve the performance of the quasi-Newton approach we provided the gradient of the posterior distribution with respect to the parameters. The relevant derivatives are given below:

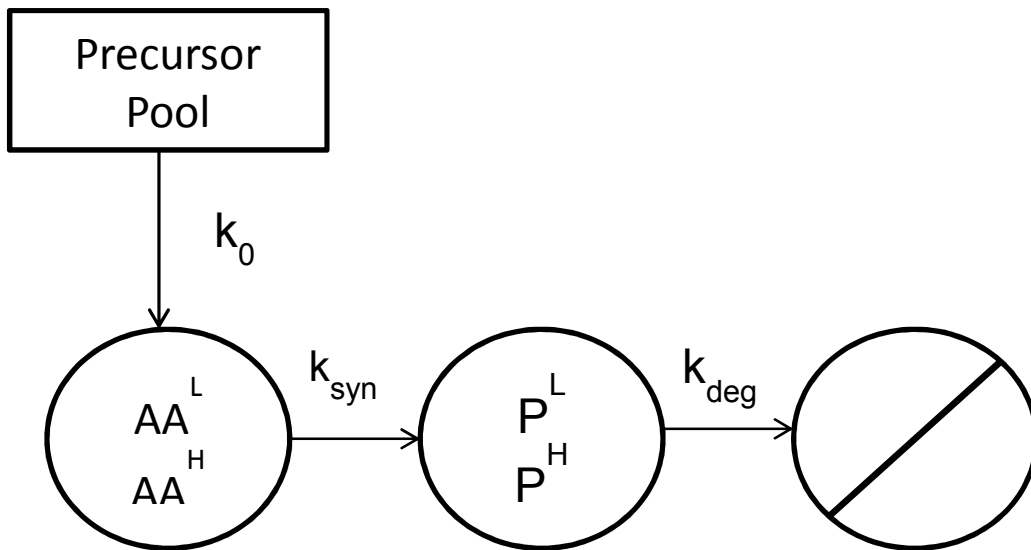
$$\begin{aligned} \frac{\partial}{\partial k_{\text{deg}}} \log(\mathcal{L}(\theta)) &= -0.5 \text{Tr} \left( \Sigma^{-1} \frac{\partial}{\partial k_{\text{deg}}} \Sigma \right) + 0.5 (\vec{y} - \vec{\mu})^T \Sigma^{-1} \left( \frac{\partial}{\partial k_{\text{deg}}} \Sigma \right) \Sigma^{-1} (\vec{y} - \vec{\mu}) + \\ &\quad + \lambda k_{\text{syn}} \left( \frac{e^{-tk_{\text{deg}}} (tk_{\text{deg}} - tk_{\text{syn}} + 1) + e^{-tk_{\text{syn}}}}{(k_{\text{syn}} - k_{\text{deg}})^2} \right)^T \Sigma^{-1} (\vec{y} - \vec{\mu}) \\ \frac{\partial}{\partial k_{\text{syn}}} \log(\mathcal{L}(\theta)) &= \lambda k_{\text{deg}} \left( \frac{e^{-tk_{\text{syn}}} (tk_{\text{syn}} - tk_{\text{deg}} + 1) + e^{-tk_{\text{deg}}}}{(k_{\text{syn}} - k_{\text{deg}})^2} \right)^T \Sigma^{-1} (\vec{y} - \vec{\mu}) \\ \frac{\partial}{\partial \sigma_{\varepsilon}^2} \log(\mathcal{L}(\theta)) &= -0.5 \text{Tr} \left( \Sigma^{-1} \frac{\partial}{\partial \sigma_{\varepsilon}^2} \Sigma \right) + 0.5 (\vec{y} - \vec{\mu})^T \Sigma^{-1} \left( \frac{\partial}{\partial \sigma_{\varepsilon}^2} \Sigma \right) \Sigma^{-1} (\vec{y} - \vec{\mu}) \\ \frac{\partial}{\partial \sigma_{\gamma}^2} \log(\mathcal{L}(\theta)) &= -0.5 \text{Tr} \left( \Sigma^{-1} \frac{\partial}{\partial \sigma_{\gamma}^2} \Sigma \right) + 0.5 (\vec{y} - \vec{\mu})^T \Sigma^{-1} \left( \frac{\partial}{\partial \sigma_{\gamma}^2} \Sigma \right) \Sigma^{-1} (\vec{y} - \vec{\mu}) \\ \frac{\partial}{\partial \lambda} \log(\mathcal{L}(\theta)) &= - \left( 1 - (k_{\text{syn}} e^{-tk_{\text{deg}}} - k_{\text{deg}} e^{-k_{\text{syn}} t}) / (k_{\text{syn}} - k_{\text{deg}}) \right)^T \Sigma^{-1} (\vec{y} - \vec{\mu}) \end{aligned}$$

In the above formula Tr stands for the trace of a matrix. The derivations use the facts, that  $\Sigma$  is dependent only on  $k_{\text{deg}}$ ,  $\sigma_{\gamma}$ ,  $\sigma_{\varepsilon}$ . Derivatives  $\Sigma$  and its determinant were obtained from the respective formulas for the matrices<sup>10</sup>. All of the derivations are in closed forms. The derivatives of the priors are added to the respective derivatives of the

log-likelihoods to obtain the partial derivatives of the log of posterior probability density function.



**A**



**B**

$$\alpha(t) = \frac{AA^H}{(AA^L + AA^H)}$$

$$\beta(t) = \frac{P^H}{(P^L + P^H)}$$

**Diagram D1.** **A** One-compartment model of protein turnover. It assumes that the proteins are synthesized at a constant rate,  $k_{\text{syn}}$ , and are degraded proportional to the protein concentration with a rate constant  $k_{\text{deg}}$ . **B** Two-compartment model assumes that proteins are synthesized from the amino acids with a rate constant,  $k_{\text{syn}}$ , and are degraded with a rate constant,  $k_{\text{deg}}$ . One- and two-compartment models result in a single and double exponential curve fits, respectively.

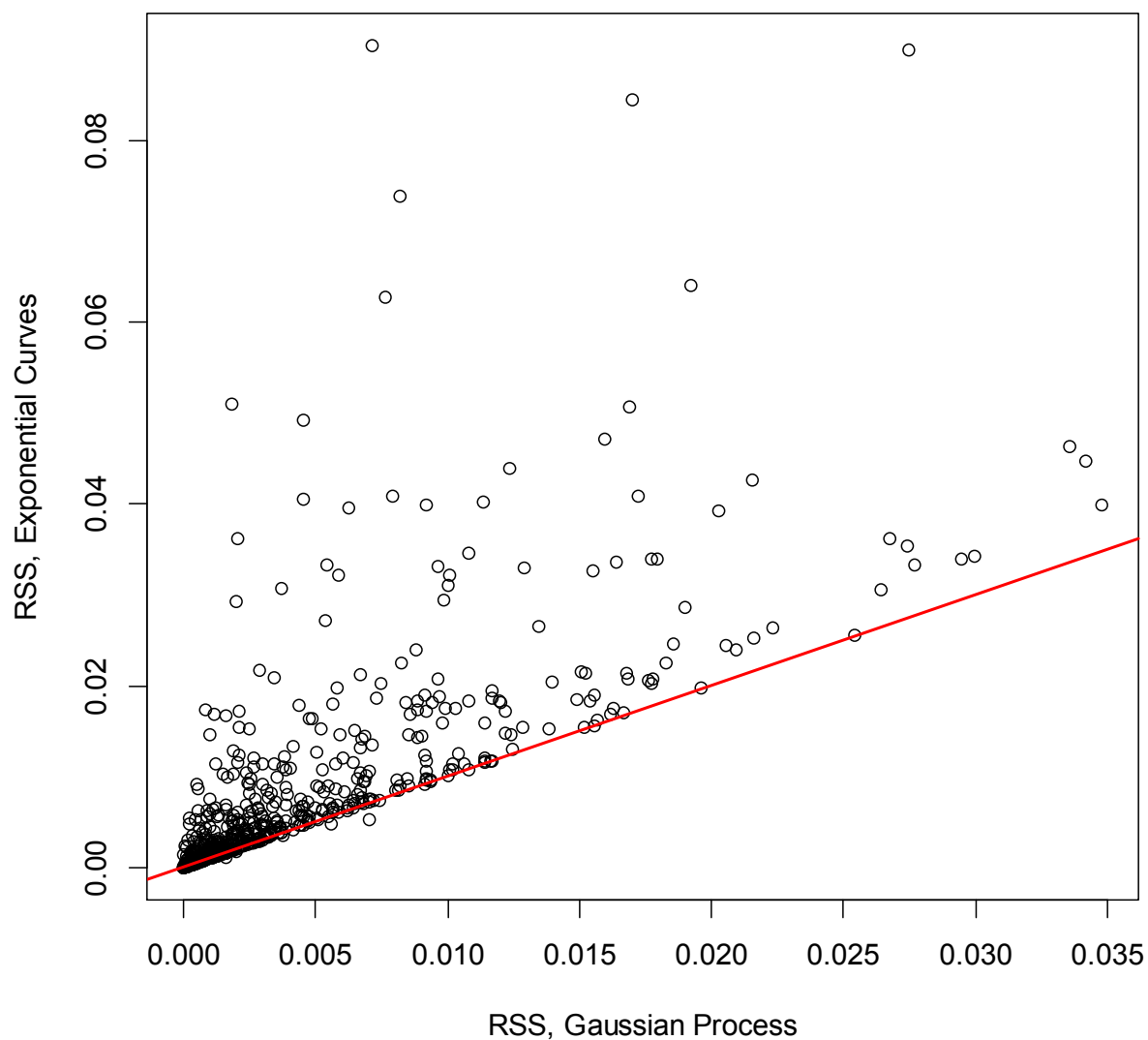


**Figure S1.** Pairwise scatter plot of the residual sum of squares obtained from protein turnover models using exponential curve fitting<sup>11</sup> (y-axis) and from GP (x-axis). The red line is the line of unity. The shown are the results for brain proteins. For 687 proteins out of 705 the GPs produced a better fit to the experimental data.

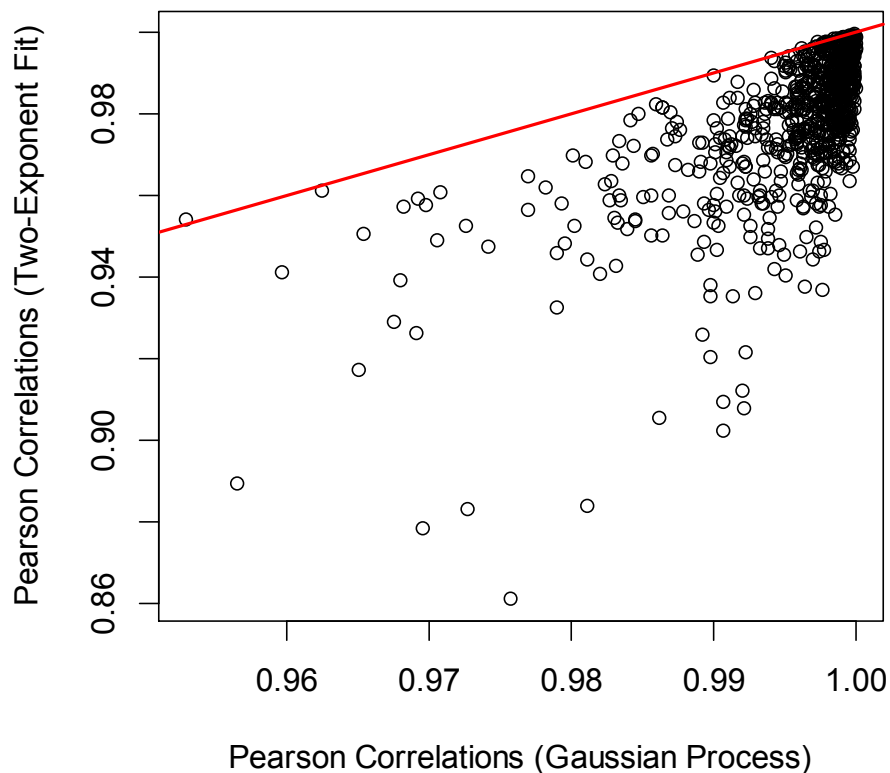


**Figure S2.** The pairwise scatter plot of the Pearson correlations obtained from protein turnover models using exponential curve fitting<sup>11</sup> (y-axis) and from GP (x-axis). The red line is the line of unity. The correlation values are those between the experimental time course data of protein labeling and predictions from a model. For 794 out of the 797 mouse liver proteins the GP produced predictions which correlated with the experimental data better than the corresponding correlations between the experimental data and two-exponent curve fit.

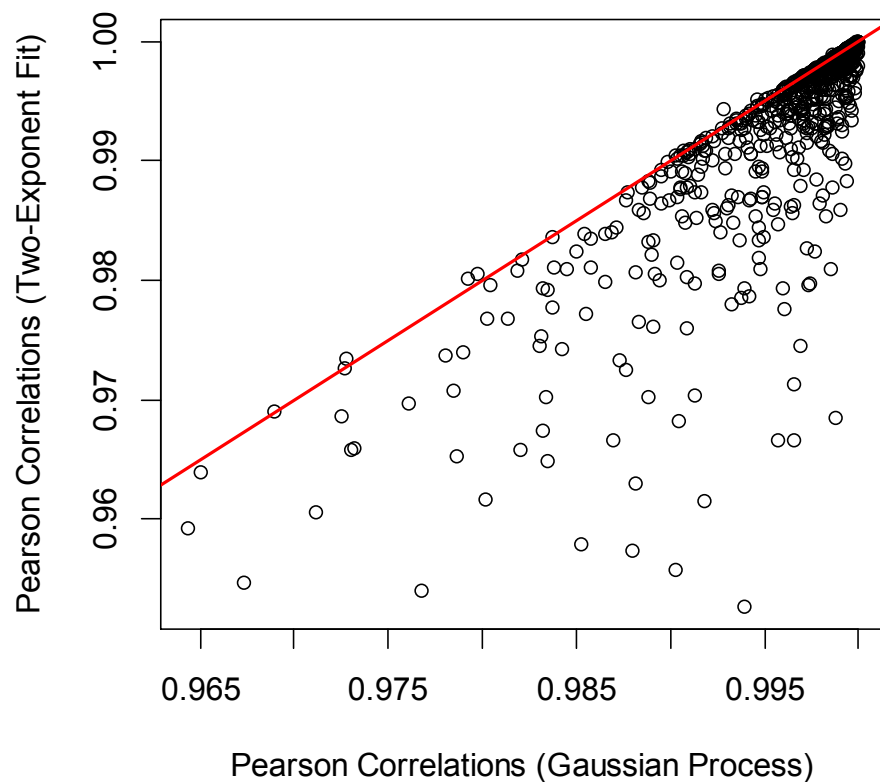


**Figure S3.** The pairwise scatter plot of the Pearson correlations obtained from protein turnover models using exponential curve fitting<sup>11</sup> (y-axis) and from GP (x-axis) for mouse brain proteins. The red line is the line of unity. The correlation values are those between the experimental time course data of protein labeling and predictions from a model. For 660 out of the 705 mouse brain proteins the GP produced predictions which correlated with the experimental data better than the corresponding correlations between the experimental data and two-exponent curve fit.



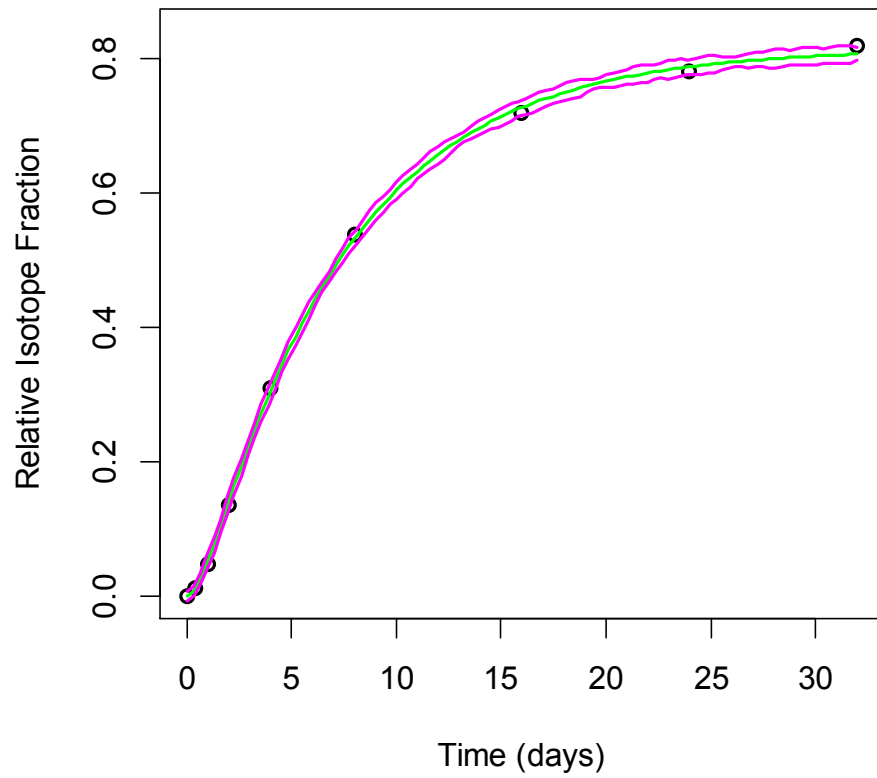


**Figure S4.** 95% confidence interval (between magenta colored lines) of the mean (green) obtained from the fit to the experimental data (empty circles) using GP with OU covariance matrix for mitochondrial trifunctional protein, subunit  $\alpha$  (Q8BMS1).

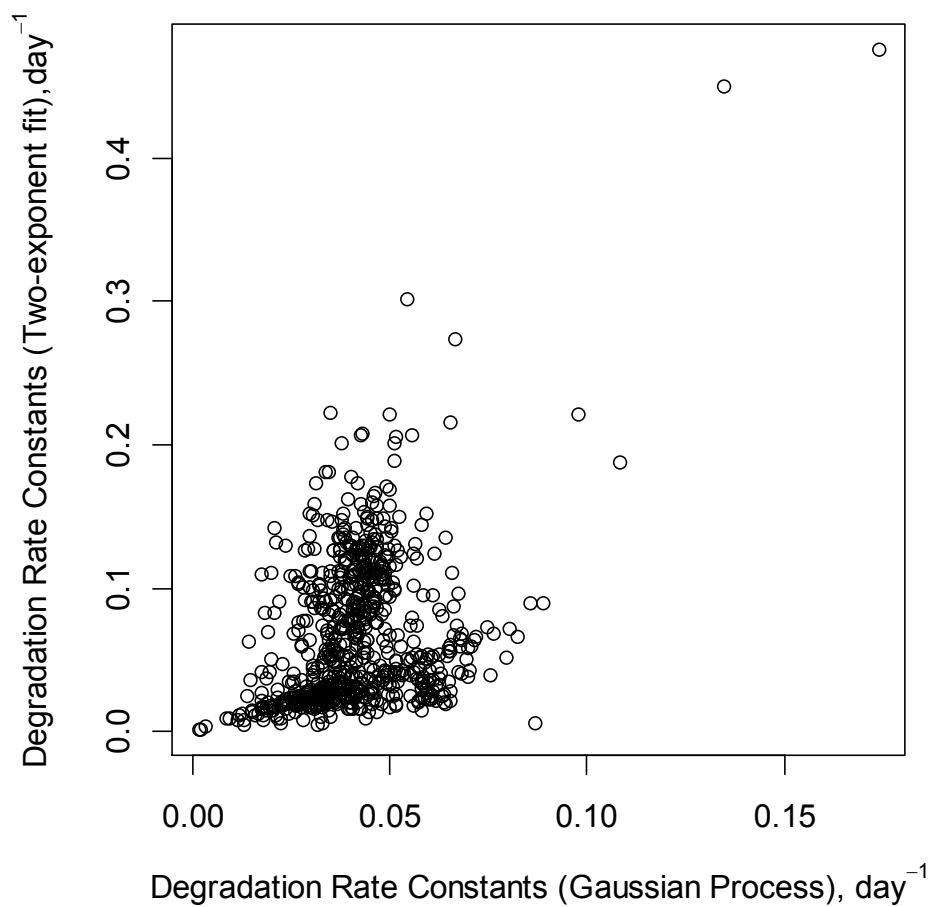


**Figure S5.** A scatter plot of the decay rates constants obtained from the GP (x-axis) and two-exponent curve fitting (y-axis). In general the rate constants computed by the GP model were larger (mouse brain proteins).

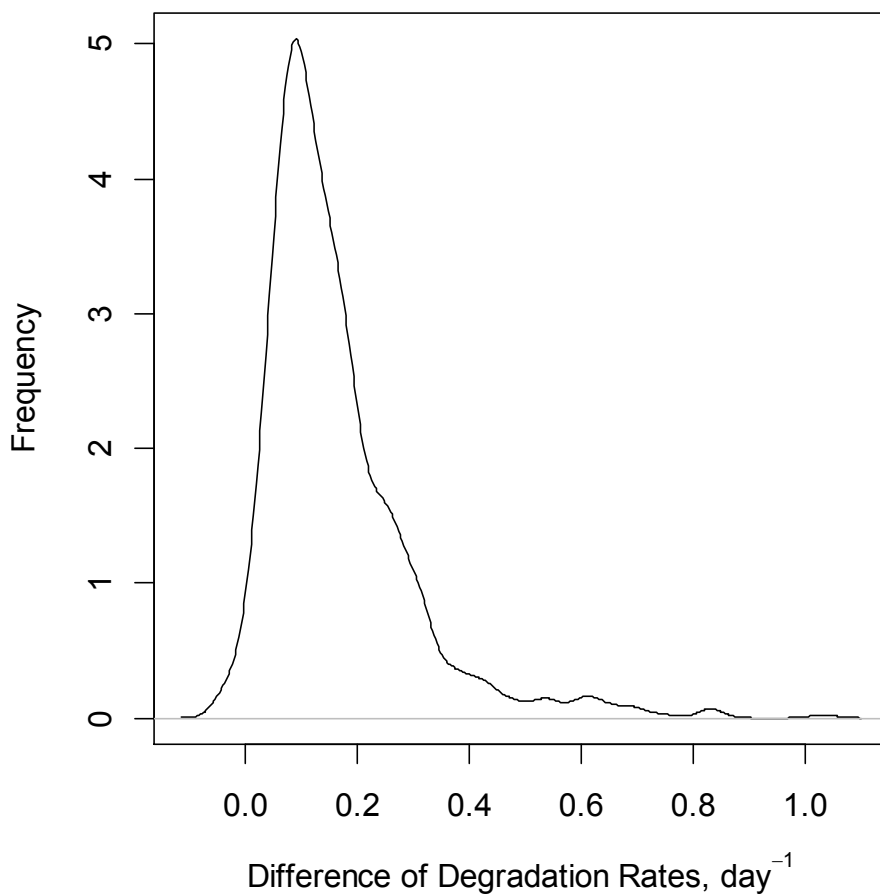


**Figure S6.** The density of the difference between degradation rate constants computed by the GP and two-exponent curve fit. The rate constants computed by the GPs were larger (faster degradation than predicted by the two-exponent curve fit).

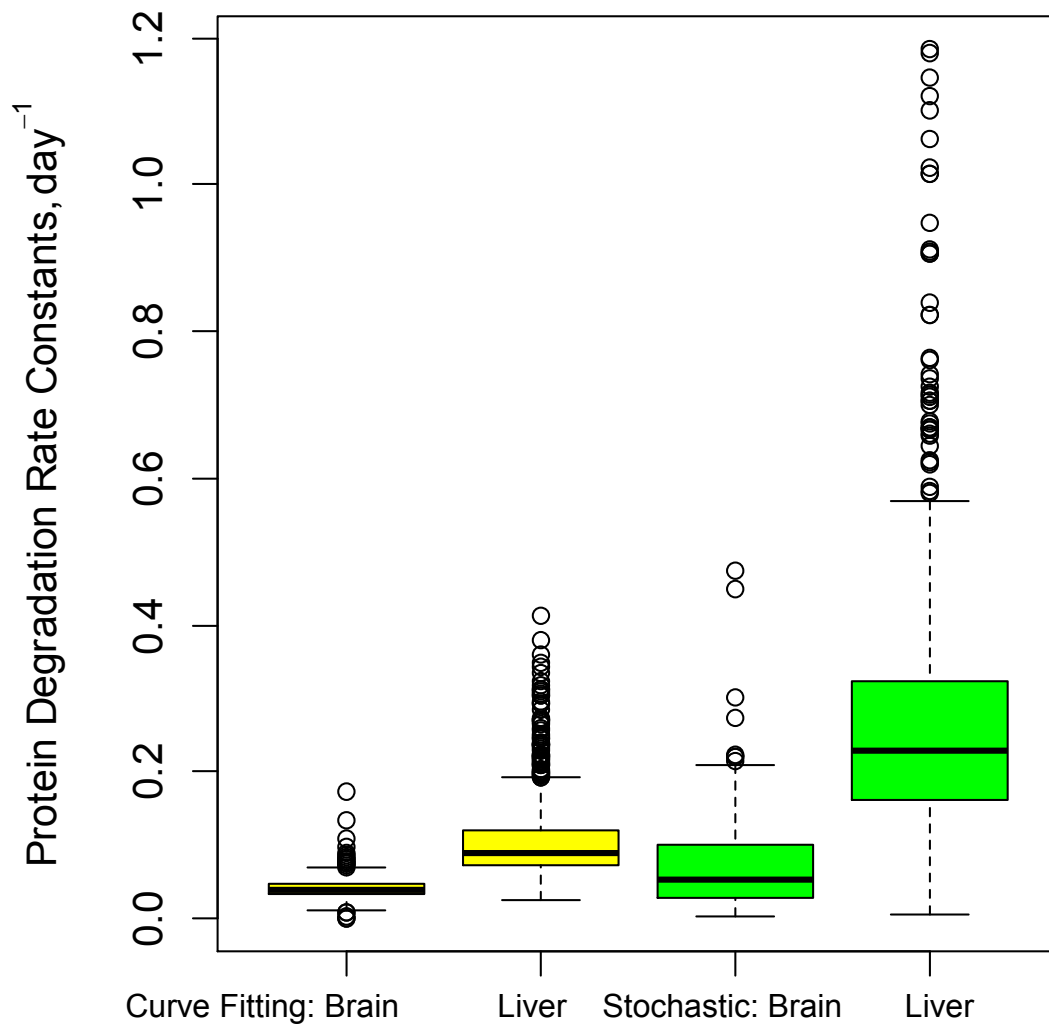


**Figure S7.** The boxplots of the decay rate constants computed by two-exponent curve fitting (yellow) and GP model (green) for mouse Brain and Liver proteomes. The latter predicts about two-fold faster degradation rate constants in mouse liver.

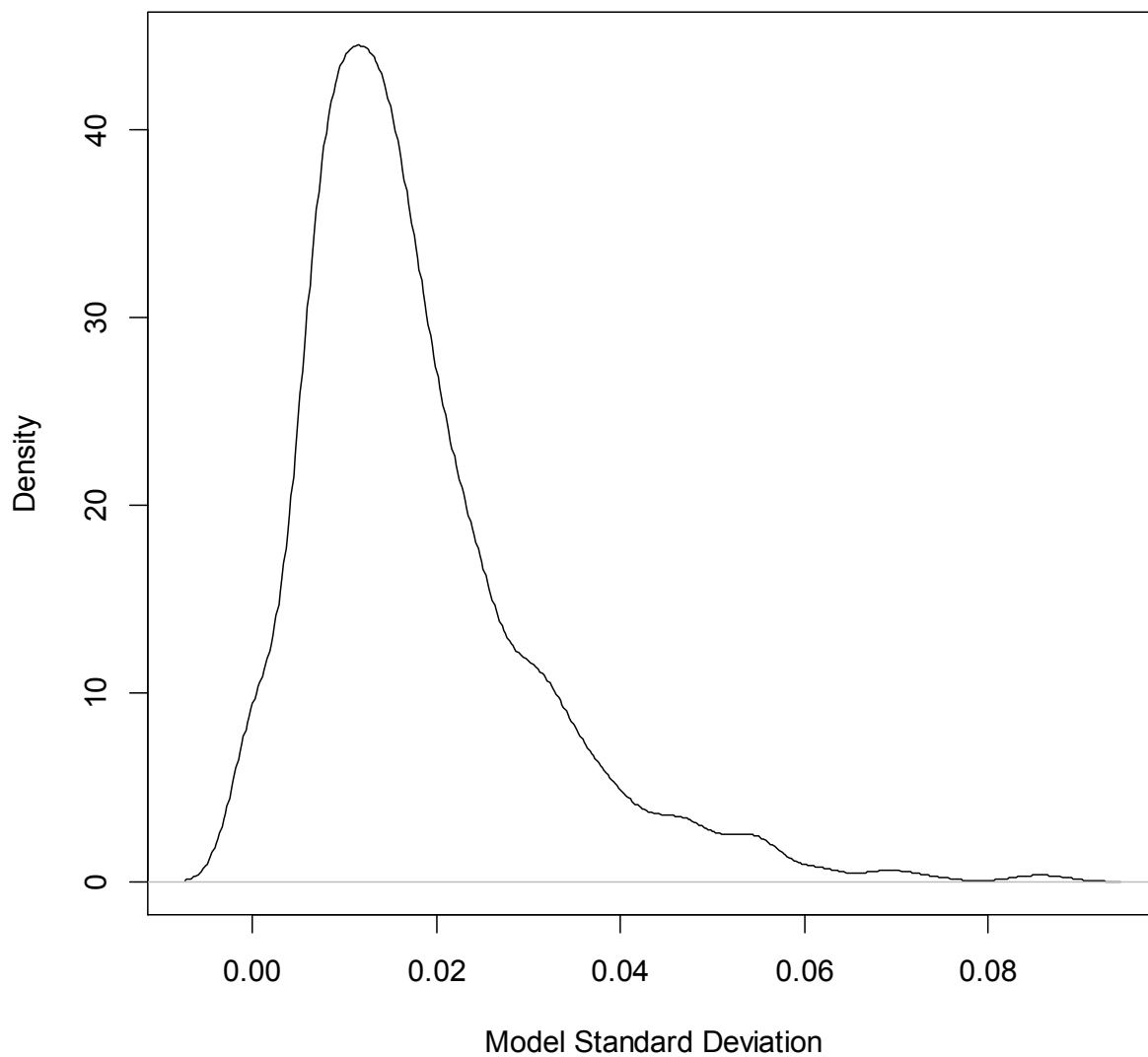


**Figure S8.** The density of standard deviations,  $\sigma_y$ , of model distributions for the liver data set.

## References

- [1] Guan, S., Price, J. C., Ghaemmaghami, S., Prusiner, S. B., and Burlingame, A. L. (2012) Compartment modeling for mammalian protein turnover studies by stable isotope metabolic labeling, *Anal. Chem* 84, 4014-4021.
- [2] Donnet, S., Foulley, J. L., and Samson, A. (2010) Bayesian analysis of growth curves using mixed models defined by stochastic differential equations, *Biometrics* 66, 733-741.
- [3] Iksendal, B. K. (2003) *Stochastic differential equations : an introduction with applications*, 6th ed., Springer, Berlin ; New York.
- [4] Iacus, S. M. (2008) Simulation and inference for stochastic differential equations with r examples, In *Springer series in statistics*, Springer,, New York, N. Y.
- [5] Aijo, T., Granberg, K., and Lahdesmaki, H. (2013) Sorad: a systems biology approach to predict and modulate dynamic signaling pathway response from phosphoproteome time-course measurements, *Bioinformatics* 29, 1283-1291.
- [6] Zhang, Y., Reckow, S., Webhofer, C., Boehme, M., Gormanns, P., Egge-Jacobsen, W. M., and Turck, C. W. (2011) Proteome scale turnover analysis in live animals using stable isotope metabolic labeling, *Anal. Chem* 83, 1665-1672.
- [7] Zurauskiene, J., Kirk, P., Thorne, T., Pinney, J., and Stumpf, M. (2014) Derivative processes for modelling metabolic fluxes, *Bioinformatics* 30, 1892-1898.
- [8] Tsai, T. H., Tadesse, M. G., Di, P. C., Pannell, L. K., Mechref, Y., Wang, Y., and Ransom, H. W. (2013) Multi-profile Bayesian alignment model for LC-MS data analysis with integration of internal standards, *Bioinformatics* 29, 2774-2780.
- [9] Byrd, R. H., Lu, P. H., Nocedal, J., and Zhu, C. Y. (1995) A Limited Memory Algorithm for Bound Constrained Optimization, *Siam J Sci Comput* 16, 1190-1208.
- [10] Bishop, C. M. (2006) *Pattern recognition and machine learning*, Springer, New York.
- [11] Guan, S., Price, J. C., Prusiner, S. B., Ghaemmaghami, S., and Burlingame, A. L. (2011) A data processing pipeline for mammalian proteome dynamics studies using stable isotope metabolic labeling, *Mol. Cell Proteomics* 10, M111.